

Probing quintessence: reconstruction and parameter estimation from supernovae

Brian F. Gerke^{1,2*} and G. Efstathiou^{1†}

¹*Institute of Astronomy, Madingley Rd., Cambridge CB3 0HA, UK*

²*Department of Physics, University of California-Berkeley, Berkeley, CA 94720, USA*

5 February 2008

ABSTRACT

We explore the prospects for using future supernova observations to probe the dark energy. We focus on quintessence, an evolving scalar field that has been suggested as a candidate for the dark energy. After simulating the observations that would be expected from the proposed SuperNova / Acceleration Probe satellite (SNAP), we investigate two methods for extracting information about quintessence from such data. First, by expanding the quintessence equation of state as $w_Q(z) = w_Q(0) - \alpha \ln(1+z)$, to fit the data, it is possible to reconstruct the quintessence potential for a wide range of smoothly varying potentials. Second, it will be possible, to test the basic properties of the dark energy by constraining the parameters Ω_Q , w_Q and α . We show that it may be possible, for example, to distinguish between quintessence and the cosmological constant in this way. Further, when supernova data are combined with other planned cosmological observations, the precision of reconstructions and parameter constraints is significantly improved, allowing a wider range of dark energy models to be distinguished.

Key words: supernovae: general – large-scale structure of Universe – cosmology: miscellaneous.

1 INTRODUCTION

There is now strong evidence, from observations of type Ia supernovae (Perlmutter et al. 1999; Riess et al. 1998) and CMB anisotropy (de Bernardis et al. 2002; Netterfield et al. 2002; Pryke et al. 2002), that we live in a universe that is geometrically flat and dominated by a nearly homogeneous component with negative pressure—the dark energy—which is causing the cosmic expansion to accelerate. The existence of dark energy has recently been confirmed, independently of the supernova data, by combining the latest galaxy clustering data with CMB measurements (Efstathiou et al., 2002; Wang, Tegmark & Zaldarriaga 2002). The most obvious dark energy candidate is vacuum energy, represented by the cosmological constant Λ , which has pressure $p_\Lambda = -\rho_\Lambda$. Other dark energy candidates, include a network of topological defects and the much-discussed possibility of quintessence (Caldwell, Dave & Steinhardt 1998), a spatially inhomogeneous, evolving component which is usually represented by a scalar field evolving in a potential (an idea first introduced by Peebles & Ratra (1988)). In this paper we will focus on quintessence, though some of the results apply to

other forms of dark energy in so far as these can be parameterised by a simple equation of state.

It is our goal to explore what could be learned about the dark energy from future observations of type Ia supernovae (SNIa), such as may be possible with the proposed SuperNova / Acceleration Probe (SNAP) satellite (Levi et al. 2000). This satellite aims to observe roughly 2000 supernovae a year for three years, with very precise magnitude measurements and negligible systematic errors, out to a redshift of $z = 1.7$. Observations of this sort will permit a very precise measurement of the magnitude-redshift relation $m(z)$ and hence of the distance-redshift relation $r(z)$, which will probe the expansion history of the universe.

Current supernova observations already put weak constraints on the dark energy density Ω_Q and equation of state w_Q . If the universe is assumed to be flat (*i.e.*, $\Omega_k \equiv 1 - \Omega_M - \Omega_Q = 0$) and w_Q is assumed to be constant in time, we have $\Omega_Q \gtrsim 0.5$ and $w_Q \lesssim -0.4$ (Perlmutter et al. 1999). These constraints improve considerably when they are combined with independent constraints from the CMB (Efstathiou 1999) or large-scale structure (Perlmutter, Turner & White 1999)—most importantly, such combined data sets give $w_Q \lesssim -0.6$.

Several studies have examined the improved parameter constraints that may be possible with SNAP. For example,

* bgerke@socrates.berkeley.edu

† gpe@ast.cam.ac.uk

2 Brian F. Gerke and G. Efstathiou

Weller & Albrecht (2001, 2002) have found that SNAP can constrain a constant w_Q to better than 10% accuracy, allowing some models to be distinguished from a cosmological constant ($w_\Lambda = -1$). In addition, many authors have examined the possibility of using SNAP to distinguish the evolution of w_Q with redshift (Astier 2001; Barger & Marfatia 2001; Goliath et al., 2001; Huterer & Turner 2001; Maor, Brustein & Steinhardt 2001; Weller & Albrecht 2001, 2002). There is a general consensus that SNAP data alone will not be able to distinguish an evolving equation of state. Our results are in broad agreement with these studies.

It may also be possible to perform a direct reconstruction of $w_Q(z)$ and of the quintessence potential V from supernova observations (Huterer & Turner 1999; Chiba & Nakamura 2000). Saini et al. (2000) have attempted to perform reconstruction from the current supernova data and find, unsurprisingly, that nothing definitive can be learned at present. The theoretical studies that have been done have often encountered difficulty in accurately reconstructing the properties of a given model from simulated supernova data (Huterer & Turner 2001; Weller & Albrecht 2002). This casts doubt upon the reliability of reconstruction. One of our main goals in the present study is to develop a reliable method for producing accurate reconstructions from supernova data that is applicable to a wide class of quintessence models. Having done this, we will also want to explore whether such reconstructions will be useful. The method we use for reconstruction demonstrates the power of using supernova observations to constrain cosmological parameters, and it highlights the usefulness of combining these observations with prior knowledge from other cosmological measurements. We therefore also undertake an exploration of the parameter constraints that will be possible with SNAP and its combination with other experiments, expanding on earlier analyses and discussing carefully what can and cannot be learned in this way.

This paper is arranged as follows. in Section 2 we summarize the cosmological effects of quintessence pertaining to supernova observations. In Section 3 we simulate SNAP-like data for a quintessence-dominated universe and discuss the problems inherent in producing reconstructions from such data. We discuss a cosmologically parameterized fitting function for $r(z)$ in Section 4, and we use it for reconstruction in Section 5. In Section 6 we show how more general questions about the nature of the dark energy may be addressed by constraining parameters with SNIa data, and we discuss the long-term prospects for this sort of study in Section 7. We draw conclusions about the prospects for observational tests of dark energy in Section 8

2 TRACKER QUINTESSENCE COSMOLOGY

We consider a scalar field (the quintessence field) Q , evolving in a potential $V(Q)$. The field will be nearly spatially smooth, and for the purposes of this study, we ignore any small inhomogeneities. The density and pressure of quintessence are given by

$$\rho_Q = \frac{1}{2}\dot{Q}^2 + V(Q) \quad (1)$$

$$p_Q = \frac{1}{2}\dot{Q}^2 - V(Q). \quad (2)$$

Quintessence is usually parameterized by its equation of state $w_Q = p_Q/\rho_Q$. Looking at equations (1) and (2), we see immediately that $w_Q \geq -1$. At late times, the coordinate distance to redshift z is given by

$$r(z) = \int_0^z \frac{dz'}{H_0 [\Omega_M(1+z')^3 + \Omega_k(1+z')^2 + \Omega_Q e^{\zeta(z')}]^{1/2}}, \quad (3)$$

where $\zeta(z) \equiv [3 \int_0^z (1+w_Q(z')) d\ln(1+z')]$. In this paper we will assume a flat ($\Omega_k = 0$) cosmology. The coordinate distance (3) is of fundamental importance since it fixes the magnitude-redshift relation probed by distant SNIa.

The evolution of quintessence models is governed by the equation of motion

$$\ddot{Q} + 3H\dot{Q} + V' = 0, \quad (4)$$

where $V' \equiv dV/dQ$. One difficulty with quintessence is that, in most cases, the initial conditions of this equation must be fine-tuned for quintessence to dominate only just at the present epoch, as is required by observations. It is possible to address this problem by using *tracker potentials* (Zlatev, Wang & Steinhardt 1999; Steinhardt, Wang & Zlatev 1999), which admit attractor-like solutions, thus allowing quintessence to exhibit identical behaviour at late times for a wide range of initial conditions. The energy scale of these models still requires fine-tuning to be consistent with observations, however (see Vilenkin (2001) for further discussion of these issues). The k -essence models (Armendariz, Mukhanov & Steinhardt 2000, 2001) also address the fine-tuning of initial conditions by adding to the quintessence Lagrangian kinetic terms that require quintessence to become dominant only after matter domination. Non-minimally coupled scalar fields offer another possible explanation of why quintessence domination might be related to the epoch of radiation and matter equality (see Bean (2001) and references therein). These models introduce extra complications with little extra motivation, however, so to keep things simple we will concern ourselves with tracker models exclusively here. We note that tracker models tend to evolve very slowly at late times, making it particularly difficult to detect evolution and reconstruct potential shapes. So by focusing on tracker models here, we should be making a conservative assessment of the prospects for testing quintessence models with supernova observations.

Inverse power-law potentials $V \propto Q^{-P}$ provide the simplest tracker quintessence models, but such models are inconsistent with the current observational constraint $w_Q \lesssim -0.6$ (Perlmutter, Turner & White 1999; Efstathiou 1999) for $P > 2$. To keep things both simple and realistic, then, we shall use a potential $V \propto Q^{-2}$ as our standard test potential in this study. [Recently it has been suggested that current observations may actually rule out all inverse-power-law models (Corasaniti & Copeland 2002; Bean & Melchiorri 2002), but they nevertheless provide a useful theoretical test model.] We shall see next how a supernova measurement of $r(z)$ can be used to probe the properties of the dark energy.

3 RECONSTRUCTING THE QUINTESSENCE POTENTIAL

Various authors (Starobinsky 1998; Huterer & Turner 1999; Nakamura & Chiba 1999) have derived equations for recon-

structing the quintessence potential $V(Q)$ and equation of state $w_Q(z)$ from $r(z)$. The equation of state of the quintessence component is given by

$$1 + w_Q(z) = \frac{(1+z)}{3} \times \frac{3\Omega_M(1+z)^2 + 2(d^2\tilde{r}/dz^2)/c^2(d\tilde{r}/dz)^3}{\Omega_M(1+z)^3 - (cd\tilde{r}/dz)^{-2}}, \quad (5)$$

and the quintessence potential is given parametrically by

$$\omega[\tilde{Q}(z)] = \left[\frac{1}{(d\tilde{r}/dz)^2} + \frac{(1+z)}{3} \frac{d^2\tilde{r}/dz^2}{(d\tilde{r}/dz)^3} \right] - \frac{1}{2}\Omega_M(1+z)^3, \quad (6)$$

$$\frac{d\tilde{Q}}{dz} = \pm \frac{d\tilde{r}/dz}{(1+z)} \times \left[-\frac{1}{4\pi} \frac{(1+z)d^2\tilde{r}/dz^2}{(d\tilde{r}/dz)^3} - \frac{3}{8\pi}\Omega_M(1+z)^3 \right]^{1/2}. \quad (7)$$

Here we follow Huterer & Turner (1999) in using the dimensionless quantities $\tilde{r} = H_0 r$, $\tilde{Q} = Q/M_{Pl}$, and $\omega(\tilde{Q}) = V(Q)/\rho_{crit} = V(\tilde{Q}M_{Pl})/(3H_0^2/8\pi G)$. Thus, in principle, a measurement of $r(z)$ will allow us to reconstruct the basic properties of quintessence.

To test reconstruction, we choose a tracker potential $V(Q)$, evolve equation (4) to obtain $w_Q(z)$ and Ω_Q , and compute the Hubble-constant-free luminosity distance $\mathcal{D}_L(z) = (1+z)\tilde{r}(z)$ from equation (3). The magnitude-redshift relation is then given by

$$m(z) = \mathcal{M} + 5 \log \mathcal{D}_L(z), \quad (8)$$

where $\mathcal{M} = M - 5 \log H_0 + 25$ is the Hubble-constant-free absolute magnitude, which we take to be $\mathcal{M} = -3.45$, the best-fit value from Efstathiou (1999). From this, we draw a Monte-Carlo sample of supernova magnitude-redshift data-points similar to what would be expected from the proposed SNAP satellite (Levi et al. 2000). Our simulated sample consists of roughly 2000 high-redshift supernovae from SNAP, in the range $0.1 \leq z \leq 1.7$, plus 200 low-redshift points from ground-based searches, in the range $0 < z \leq 0.2$. The points have a measurement error of 0.01 magnitude, plus an intrinsic scatter (Efstathiou et al. 1999) of 0.018 magnitude after correction for the decline rate-luminosity correlation. The error in the redshift is negligible, and the redshift distribution we use, (Fig. 1), is similar to the one used by Huterer & Turner (2001). We neglect systematic errors in this analysis.

Given our set of N datapoints, we next choose a fitting function $\tilde{r}^{fit}(z)$. For a grid of points in the parameter space of $\tilde{r}^{fit}(z)$ we compute the likelihood function

$$\mathcal{L} = \prod_{i=1}^N \frac{1}{\sqrt{2\pi\sigma_i^2}} \exp \left[-\frac{(m_i - m^{fit}(z_i))^2}{2\sigma_i^2} \right], \quad (9)$$

where m_i is the magnitude of datapoint i , z_i is its redshift, and σ_i is the error. The magnitude predicted by the fitting function is given by $m^{fit}(z) = \mathcal{M} + 5 \log \mathcal{D}_L^{fit}(z)$. For the points in parameter space that fall within the 68%, 95% and 99% confidence regions, we use $\tilde{r}^{fit}(z)$ to reconstruct $w_Q(z)$ and $V(Q)$ from equations (5–7). We then draw confidence contours around the outermost reconstructed curves from each confidence region.

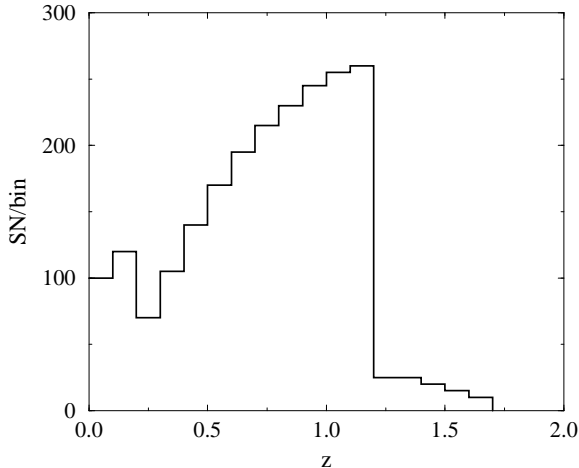


Figure 1. The expected redshift distribution of supernovae observations from the SNAP satellite (Levi et al. 2000), augmented by ground-based low-redshift observations. This distribution is similar to that given in Huterer & Turner (2001).

It is important to note here a basic mathematical difficulty with reconstruction. Looking at equation (7), we see that reconstruction of $V(Q)$ is impossible when the expression in square brackets crosses zero. When this occurs at a given confidence level, we terminate the corresponding reconstruction contour for $V(Q)$. Also, we note that the present-day value of the quintessence field Q is not fixed by equation (7). But since this value has no cosmological effect, we may arbitrarily set $Q = 1$ at the present day.

Various functional forms for $\tilde{r}^{fit}(z)$ have been recommended in the literature for use in reconstruction (Huterer & Turner 2001; Weller & Albrecht 2002; Chiba & Nakamura 2000; Saini et al. 2000). To show the difficulties inherent in reconstruction, we attempt reconstructions using two of them—a third order polynomial

$$\tilde{r}^{fit}(z) = a_3 z^3 + a_2 z^2 + a_1 z, \quad (10)$$

and a Padé approximate

$$\tilde{r}^{fit}(z) = \frac{z(1+az)}{1+bz+cz^2}, \quad (11)$$

both of which have been suggested by Huterer & Turner (1999, 2001). Reconstructions resulting from fitting SNAP-like data with these fitting functions are shown in Fig 2. In applying the reconstruction equations here, we have assumed that Ω_M is known exactly. Evidently, the precision of the reconstructions will diminish if we allow for some uncertainty in Ω_M .

The reconstructions we obtain are inaccurate. For the polynomial fit, the actual value of w_Q lies outside the 99% confidence contour at low redshift, where the reconstruction is most precise, and the actual value of $V(Q)$ lies outside the 68% contour at high values of Q . The Padé fit does significantly better, but the reconstruction of $w_Q(z)$ is still slightly inaccurate at low z . Reconstructions based on these fitting functions thus appear to be unreliable. Since our reconstruction contours rule out the *correct* model, we cannot

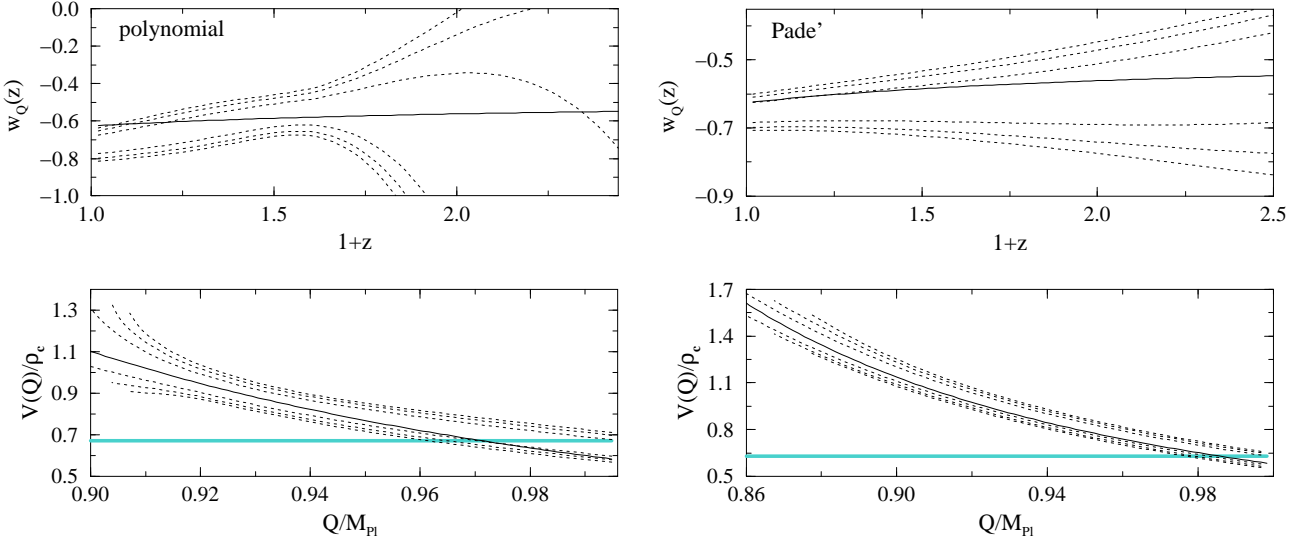


Figure 2. Reconstruction of $V(Q)$ and $w_Q(z)$ for a quintessence model with $V \propto Q^{-2}$. In the left-hand panels we have used the third-order polynomial (10) as a fitting function, and in the right-hand panels we have used the Padé approximate (11). The dashed lines—from innermost to outermost pairs—are 68%, 95% and 99% confidence contours, and the solid black lines are the actual model values. The heavy lines in the lower panels are lines of constant V , for reference. Inaccuracies in the derivatives of the fitting functions lead to inaccurate reconstructions of $w_Q(z)$ and, for the polynomial fit, of $V(Q)$.

seriously claim that they rule out *any* specific model: they are too inaccurate to be useful. (Similar difficulties with the 3rd-order polynomial fit were noted by Weller & Albrecht (2002) in a preprint which appeared as this work was being completed.)

This difficulty arises because the reconstruction equations (5–7) depend on the derivatives of $\tilde{r}(z)$, rather than on $\tilde{r}(z)$ itself, but the derivatives of the fitting functions do not necessarily resemble the derivatives of $r(z)$. (This problem has also been noted by Huterer & Turner (2001) and Weller & Albrecht (2002).) The problem with the fitting functions suggested in the literature is that, with the exception of the one in Saini et al. (2000), they are all arbitrary functions that have been chosen because they give good fits to $\tilde{r}(z)$. However, we have no *a priori* reason to believe that their derivatives will resemble $d\tilde{r}/dz$ and $d^2\tilde{r}/dz^2$. Indeed, as Fig. 3 shows, the best fitting polynomial and Padé approximate do not provide particularly accurate fits to the derivatives of $r(z)$. Therefore we should not expect to obtain accurate reconstructions from these functions. To perform reconstructions reliably, we must first find a fitting function that we believe will provide not only a good fit to $\tilde{r}(z)$, but also a good approximation to its derivatives. In essence, we want to fit our data with some physically motivated approximation to $\tilde{r}(z)$.

4 A PHYSICALLY MOTIVATED FITTING FUNCTION

We can construct a physically motivated fitting function by noting that, for low z , the quintessence equation of state is often well approximated by

$$w_Q^{app} = w_Q(a_0) + \alpha \ln(a/a_0) = w_Q(z=0) - \alpha \ln(1+z), \quad (12)$$

where $\alpha \equiv dw_Q/d \ln a$ (Efstathiou 1999). Combining this with equation (3), we arrive at an approximate expression for the coordinate distance, which we can use as a fitting function for reconstruction:

$$\tilde{r}^{fit}(z) = \int_0^z \frac{dz'}{\left[\Omega_M(1+z')^3 + \Omega_Q^{app}(z')\right]^{1/2}}, \quad (13)$$

where the approximate energy density contribution of the quintessence component is

$$\Omega_Q^{app}(z) = \Omega_Q(1+z)^{3(1+w_Q(0))} \exp\{-(3/2)\alpha[\ln(1+z)]^2\}. \quad (14)$$

Also, by assumption, $\Omega_M = 1 - \Omega_Q$ (present-day values). Equation (13) is readily twice differentiable with respect to z ; hence it can be used to reconstruct $V(Q)$ and $w_Q(z)$. A similar fitting function [with a linear, rather than logarithmic, approximation to $w_Q(z)$] has been found to provide the best fits to $r(z)$ of any of the fitting functions previously considered in the literature (Weller & Albrecht 2001). Fig. 3 shows that equation (13) also produces better fits to $d\tilde{r}/dz$ and $d^2\tilde{r}/dz^2$ than the polynomial or Padé approximate, suggesting that it may produce reliable reconstructions. This is entirely to be expected, since the fitting function is a direct approximation to the coordinate distance in terms of real physical parameters. Of course this function will produce reliable reconstructions only to the extent that it is a good approximation to $\tilde{r}(z)$, but we expect that it will approximate $\tilde{r}(z)$ reasonably well, for a wide range of quintessence models, out to at least the redshifts to be probed by SNAP (Efstathiou 1999). It is worth noting that some models will not be well approximated by equation (13)—for example, the pseudo-Nambu-Goldstone boson potentials considered by Weller & Albrecht (2002) (which can produce an oscillatory equation of state) would generally require a more complicated fitting function. Nevertheless, the analy-

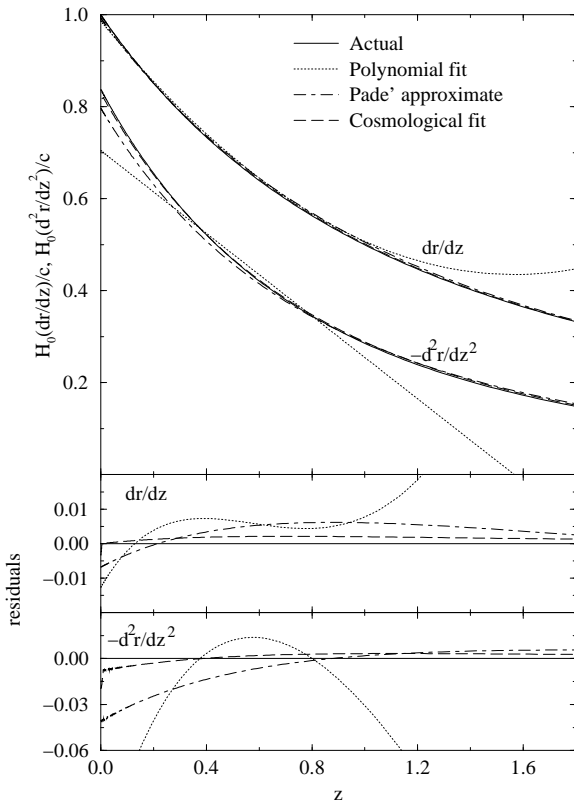


Figure 3. Derivatives of the best fits to $r(z)$ for various fitting functions, compared with the actual derivatives dr/dz and d^2r/dz^2 (solid lines). The third-order polynomial fit [equation (10), dotted lines], despite producing a good fit to $r(z)$, gives an obviously poor fit to the derivatives. It will therefore produce poor reconstructions of $V(Q)$ and $w(z)$. The Padé approximate fit [equation (11), dot-dashed lines] provides more reasonable derivatives, but the small discrepancies between the fit and the actual derivatives still lead to inaccuracies in reconstruction. The fit based on a cosmological parameterization [equation (13), dashed lines] provides the best fits to dr/dz and d^2r/dz^2 , as may be expected, since the fitting function here is an approximation to the actual coordinate distance.

sis presented here is self-consistent: as long as equation (13) provides an acceptable fit to the data (reduced χ^2 of order unity), we are unlikely to learn anything more by introducing more complicated fitting functions. If there are significant residuals about the best fit, however, it may be fruitful to consider more complicated functions.

It is also important to note that the use of equation (13) as a fitting function effectively reduces the problem of reconstruction to one of constraining the cosmological parameters Ω_Q , $w_Q(0)$ and α by likelihood analysis. Parameter estimation and reconstruction are separately interesting: the former can tell us about the basic properties of dark energy in a model-independent way, whereas the latter can tell us more specifically about the potential of a scalar-field quintessence. Since we are constraining some cosmological parameters in the reconstructions discussed here, it may be possible to combine supernova observations with other observations to

better constrain the fit parameters and simultaneously to improve our reconstructions. For example, in a flat universe (which we assume), measurements of Ω_M from, *e.g.*, galaxy clustering and the CMB fix Ω_Q via the constraint equation $\Omega_Q = 1 - \Omega_M$. If there are degeneracies between the parameters, then combining such measurements with supernova data will serve to tighten the constraints on all the parameters, improving the precision of our reconstructions. Because we have used physical quantities to parameterize our fitting function for the coordinate distance, we can learn about $r^{fit}(z)$ indirectly from data other than the SN1a observations. In this way, a physically motivated fitting function allows reconstructions that are not only more accurate but also possibly more precise than reconstructions from more arbitrary fitting functions.

Fig. 4 shows the sort of constraints on Ω_Q , $w_Q(0)$ and α that might be expected from one year of SNAP data (2200 SN). Clearly, strong and complicated degeneracies between the parameters make precise constraints impossible when we use the supernova data alone for estimation. It may be possible to reduce these degeneracies significantly if we combine the supernova data with other measurements of the cosmological parameters. For example, galaxy clustering measurements from the 2dF galaxy redshift survey, combined with measurements of CMB anisotropies, constrain Ω_M to within roughly ± 0.1 (2σ errors) in the case of a flat universe (Efstathiou et al. 2002). To show the effect that such other measurements can have, we impose a Gaussian prior probability distribution on $\Omega_M = 1 - \Omega_Q$. Its effect on the contours, for various values of the standard deviation σ_{Ω_M} , is shown in Fig. 4. Clearly the use of such a prior is significant: if we impose $\sigma_{\Omega_M} = 0.05$, it is possible to constrain $w_Q(0) \neq -1$ with 99% confidence, indicating that the dark energy is not a cosmological constant. Other authors (Astier 2001; Barger & Marfatia 2001; Goliath et al. 2001; Huterer & Turner 2001; Maor et al. 2001; Weller & Albrecht 2001, 2002) have attempted to constrain a similar set of parameters using a SNAP-like dataset (using $w_1 \equiv dw_Q/dz$ where we have used $\alpha \equiv d \ln w_Q / d \ln a$). They also find that strong degeneracies between parameters make precise estimation impossible, unless prior knowledge of one of the parameters is assumed. Our results are in good agreement with these analyses.¹

But is our Gaussian prior with $\sigma_{\Omega_M} = 0.05$ realistic? The prior assumes that we will be able to measure Ω_M to this accuracy independent of the equation of state, that is, that the measurement of Ω_M does not suffer from degeneracies with w_Q . In fact, measurements of $\Omega_M h$ from the Sloan Digital Sky Survey (SDSS), combined with measurements of $\Omega_M h^2$ from the MAP satellite's CMB measurements will be able to constrain Ω_M to nearly ± 0.05 , with no dependence on w_Q (Eisenstein et al. 1998). Moreover, if flatness is assumed and this measurement is combined with measurements of the angular diameter distance to last scattering from the the MAP or Planck satellites, the uncertainty in

¹ Recently, other authors (Wang & Garnavich 2001; Wang & Lovelace 2001) have suggested, interestingly, that better information about dark energy may be obtained by constraining the function $f(z) = e^{\zeta(z)}$ (where $\zeta(z)$ is as defined after equation (3)) at various values of z , rather than by attempting to parameterize and constrain $w(z)$.

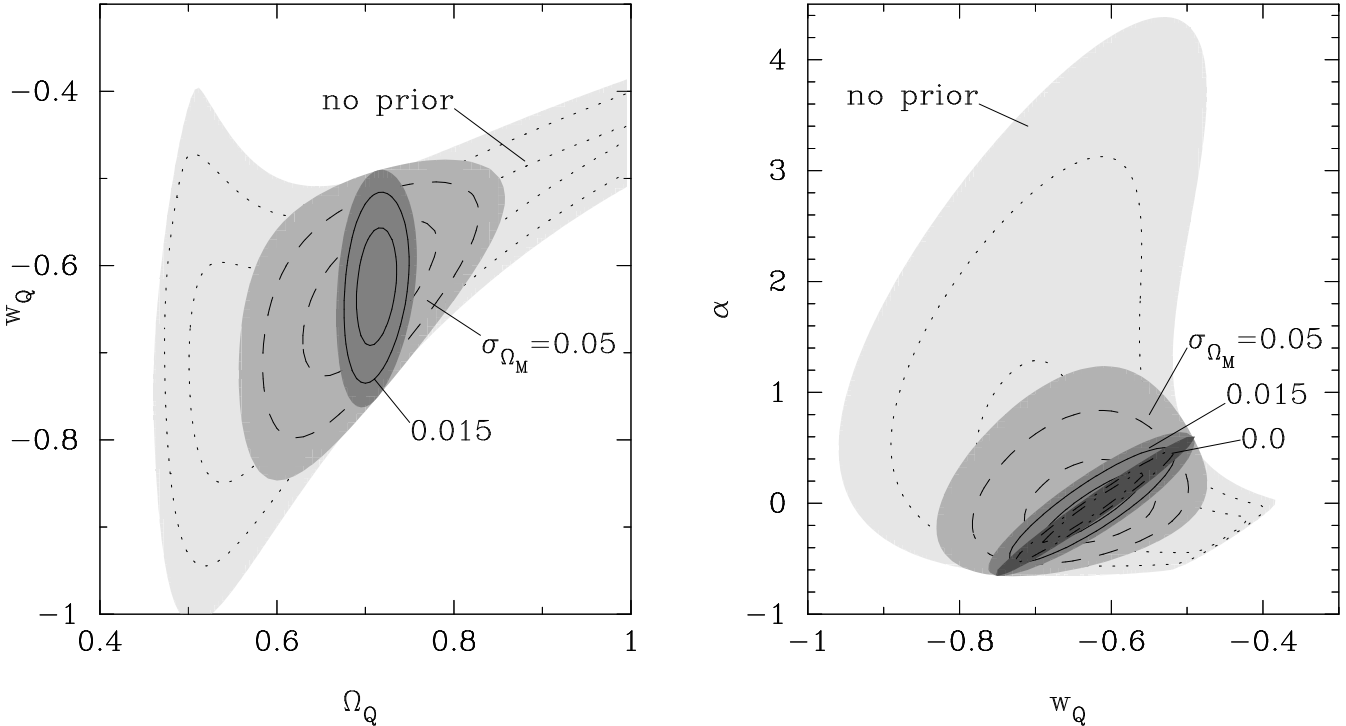


Figure 4. Likelihood contours for the cosmological parameters Ω_Q , $w_Q(0)$ and α , as defined in equation (13). The contours are calculated from a SNAP-like dataset for one year of observation, drawn from a quintessence model with $V(Q) \propto Q^{-2}$. The shaded regions indicate 99% confidence regions, given various Gaussian prior probability distributions on $\Omega_M = 1 - \Omega_Q$, with standard deviation σ_{Ω_M} . The contour lines inside each shaded region indicate the associated 95% and 68% confidence levels. Note that strong degeneracies between parameters make precise parameter estimation impossible in the absence of prior knowledge. In each graph, the two-dimensional likelihood contours shown are marginalized over the third parameter.

Ω_M decreases to 0.01–0.03, with an additional strong constraint on w_Q and no degeneracy between the parameters (Hu et al. 1998). In addition, proposed X-ray or Sunyaev-Zeldovich effect surveys of galaxy clusters can constrain Ω_M to within an error of 0.05 or better, with only a very slight dependence on w_Q (Haiman, Mohr & Holder 2001; Weller, Battye & Kneissl 2001). A proposed gravitational lensing survey could constrain Ω_M to within 0.015 with minimal w_Q dependence (van Waerbeke, Bernardeau & Mellier 1999).

The uncertainty $\sigma_{\Omega_M} = 0.05$ thus appears to be a conservative estimate of the precision that may be obtained in the future. More optimistically, we could use a prior with $\sigma_{\Omega_M} = 0.015$. Fig. 4 shows the constraints that are possible in this case: with improved knowledge of Ω_M we can also obtain much tighter constraints on $w_Q(0)$ and α . In no case is it possible to show that $\alpha \neq 0$, however, even if Ω_M is known exactly. Nevertheless, it is clear that combining SNAP parameter constraints with other measurements will be a powerful probe of the dark energy. We shall explore this in more detail below.

5 RECONSTRUCTION FROM COSMOLOGICALLY MOTIVATED FITTING FUNCTIONS

Prior knowledge of the parameters is also necessary if we are to use equation (13) successfully for reconstruction. If we impose no prior probability distribution on our likelihood

analysis (the ‘‘no prior’’ case in Fig. 4), then reconstruction of $V(Q)$ fails for nearly all Q at all confidence levels, and $w_Q(z)$ is only very weakly constrained. If, on the other hand, we impose a Gaussian prior with $\sigma_{\Omega_M} = 0.05$, we obtain the potentially useful reconstructions shown in Fig. 5. (Note that because we are explicitly constraining Ω_Q —and hence Ω_M , which appears explicitly in the reconstruction equations—we have allowed Ω_M to vary over its allowed range in applying the reconstruction equations.) In particular, $V(Q)$ is constrained to be non-constant at the 68% confidence level. More importantly, the reconstructions are accurate: both the actual $V(Q)$ and the actual $w_Q(z)$ curves are contained within the 68% confidence contours. This is very promising: it should be possible, by combining SNAP data with expected measurements of Ω_M , to reconstruct the potential of an inverse-power-law quintessence model in an accurate and reliable way.

Fig. 6 shows a reconstruction using the more optimistic prior $\sigma_{\Omega_M} = 0.015$. In this case, we are able to constrain $V(Q)$ to be non-constant at greater than 99% confidence with good accuracy, and we achieve impressive constraints on $w_Q(z)$, although it is not possible to show that $w_Q(z)$ is evolving. Because the reconstructions we obtain are accurate, it appears that equation (13) is a better fitting function for reconstruction than the arbitrary fitting functions we tried previously. But we cannot be entirely sure of this yet: when we attempted reconstructions with the polynomial and Padé approximate, we assumed exact knowledge

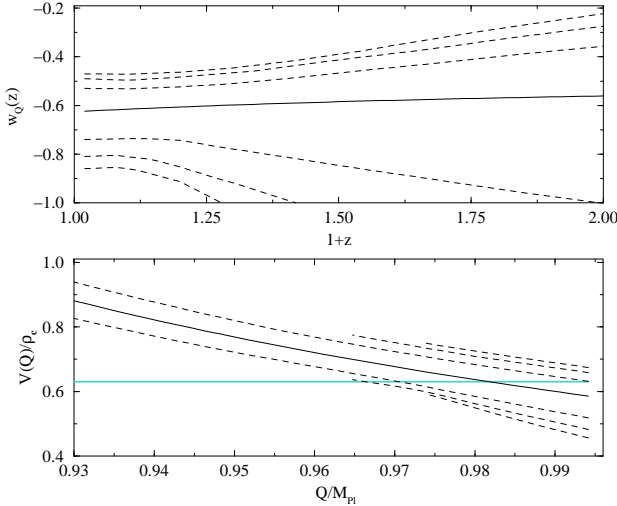


Figure 5. Reconstruction of $V(Q)$ and $w_Q(z)$ for a quintessence model with $V \propto Q^{-2}$, using equation (13) as a fitting function. A Gaussian prior is imposed on Ω_M , with standard deviation $\sigma_{\Omega_M} = 0.05$ about the actual value. Both w_Q and V are accurately constrained, and we are able to constrain $V(Q) \neq \text{const}$ at 68% confidence.

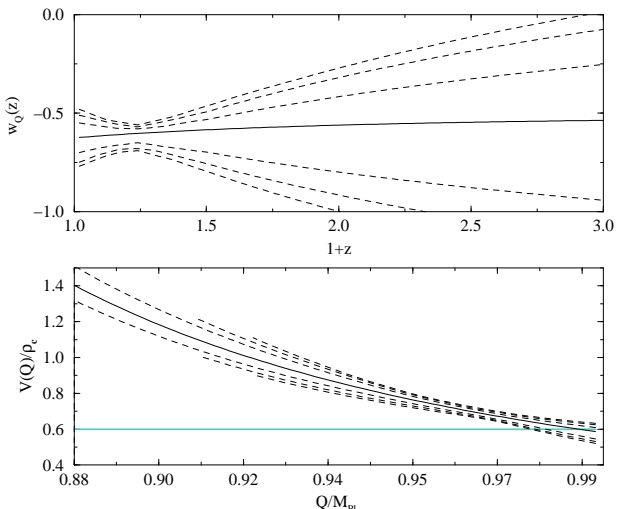


Figure 6. Similar to Fig. 5, except here $\sigma_{\Omega_M} = 0.015$. $V(Q)$ is constrained to be non-constant at $> 99\%$ confidence and $w_Q(z)$ is constrained with good precision.

of Ω_M . It is possible that our allowing Ω_M to vary here might be obscuring inaccuracies. To test this, in Fig. 7 we perform a reconstruction from equation (13), in which we hold Ω_M (and thus Ω_Q) constant at its true value throughout. The reconstructions are entirely acceptable: no obvious inaccuracies creep in when we fix Ω_M . As hoped, the use of a physically motivated fitting function has given us a method for reconstructing the properties of quintessence in an accurate and reliable way.

We note that Huterer & Turner (2001) (HT00) have previously attempted to constrain $w_Q(z)$ using a fitting function based on $w_Q^{app}(z)$. Our work differs in several important

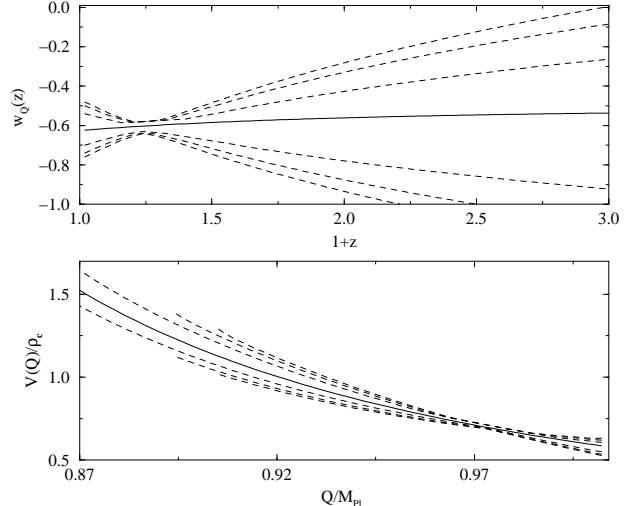


Figure 7. Similar to Fig. 5, except here we hold Ω_M fixed at its true value, rather than allowing it to vary. The fact that the reconstructions are accurate in this case indicates clearly that the cosmological fitting function (13) is a better fitting function for reconstruction than the arbitrary ones we tried previously.

respects from their analysis. First, we show here that equation (13) produces good reconstructions of $V(Q)$ as well as $w_Q(z)$. Second, whereas HT00 hold Ω_M fixed in their analysis, we show that good reconstructions are still possible when there is some uncertainty in Ω_M . Third, HT00 use the Fisher matrix to draw their confidence contours, while we use an exact likelihood analysis. Most importantly, HT00 draw their simulated data from a model with w_Q exactly equal to w_Q^{app} , which guarantees an accurate reconstruction (since the fitting function is the same as the original model). We show here that accurate reconstructions can be done even when w_Q^{app} is only an approximation to the actual equation of state. Weller & Albrecht (2002) have recently had some success in reconstructing $w_Q(z)$ using a polynomial expansion of $w_Q(z)$ to produce a fitting function, although they have also held Ω_M fixed. Also, since the equation of state is not usually well approximated by a linear function of z , they must expand w_Q to second order to obtain accurate reconstructions, which requires one more fit parameter than our fitting function. We expect that this will lead to worse degeneracies in parameter space and that it may be difficult to obtain a useful reconstruction if Ω_M is allowed to vary.

So it appears that, by fitting our data to equation (13), we have found a way to reconstruct $V(Q)$ and $w_Q(z)$ in a reliable, accurate and fairly precise way. Recall, however, that, in deriving equation (13), our basic approximation was to write the equation of state in the form $w_Q^{app}(z) = w_Q(0) - \alpha \ln(1+z)$. So what we are actually reconstructing when we use equation (13) as a fitting function is the $w_Q(z)$ that *would be* most likely to produce the data if $w_Q(z)$ had the form of $w_Q^{app}(z)$. Likewise, the $V(Q)$ that we reconstruct is the potential that *would have* produced this most likely $w_Q^{app}(z)$. If we are careful to take these issues into account, it will be possible to make use of our reconstructions to distinguish between different quintessence models. As long as $w_Q(z)$ is well approximated by $w_Q^{app}(z)$

over the redshifts we are measuring (*i.e.*, as long as it is not dominated by nonlinear terms in $\ln[1+z]$), we expect that our reconstructions will be accurate. Clearly models with rapidly varying $w_Q(z)$ (*e.g.*, the pseudo-Nambu-Goldstone boson models discussed by Weller & Albrecht (2002)) will not be accurately reconstructed using equation (13), but in these cases we also would not expect an acceptable fit to the data.

If we want to compare a given potential $V(Q)$ to our reconstructions, we must first determine whether the $w_Q(z)$ arising from it is well approximated by $w_Q^{app}(z)$. If it is not well approximated, we can say nothing useful about that particular potential using our reconstructions, since we cannot be sure that reconstructions of it would be accurate. If, on the other hand, the model in question is well approximated by $w_Q^{app}(z)$, we can determine whether it is allowed by the data. First, we vary the parameters of the potential $V(Q)$, including the present-day value of the field Q_0 , since this is not fixed by the reconstruction equations. If we do not find any parameterization that falls entirely within the reconstruction contours, then the model under consideration is disallowed by the data. If, on the other hand, we do find a satisfactory parameterization, we must then additionally check whether or not the resulting equation of state falls within the reconstruction contours for $w_Q(z)$ for the redshift range of the data. If it does not, then the model is ruled out. Any model that passes both of these tests is consistent with the data.

As an example, we test an inverse-power-law model with $V \propto Q^{-3}$ against the contours shown in Fig. 6 (recall that these arose from a quintessence model with $V \propto Q^{-2}$). We vary the parameters M and Q_0 for the potential $V(Q) = M^7/[Q - (1 - Q_0)]^3$ and identify a range of M and Q_0 for which the potential falls within the 68% confidence contours. This gives us a minimum and maximum allowed value for M . We then evolve the quintessence field in the potential $V(Q) = M^7/Q^3$, to get $w_Q(z)$ curves for both of these values. (The transformation $Q \rightarrow Q - (1 - Q_0)$ has no cosmological effect.) For inverse-power-law models w_Q decreases monotonically with increasing M ; therefore, all allowed potentials will have $w_Q(z)$ values that fall between these two limiting curves. As Fig. 8 shows, $w_Q(z)$ falls outside the 99% confidence contours for all allowed values of M , and so models with $V \propto Q^{-3}$ are ruled out by the data. The reason that the allowed potentials do not lead to allowed $w_Q(z)$ curves here is that the calculation is not self-consistent. Each allowed parameterization of $V(Q)$ includes a specific value for both M and Q_0 , but only M has any effect on the evolution of the quintessence field. For each allowed value of M , if the quintessence field does not evolve to the associated Q_0 at the present epoch, the resulting $w_Q(z)$ may still be disallowed.

Reconstructions using the fitting function equation (13) are thus clearly more useful than reconstructions using arbitrary fitting functions. Using this equation, it is possible to determine, in a consistent way, whether or not a particular model is ruled out by the data—so long as $w_Q^{app}(z)$ is a good approximation to $w_Q(z)$ for that model. With the polynomial and Padé approximate fitting functions we tried before, we would have no reliable way of ruling out specific models, since we would have no good way of determining whether the fitting function accurately approximates the derivatives of \tilde{r} . Any apparent conclusion from arbitrary fitting functions like

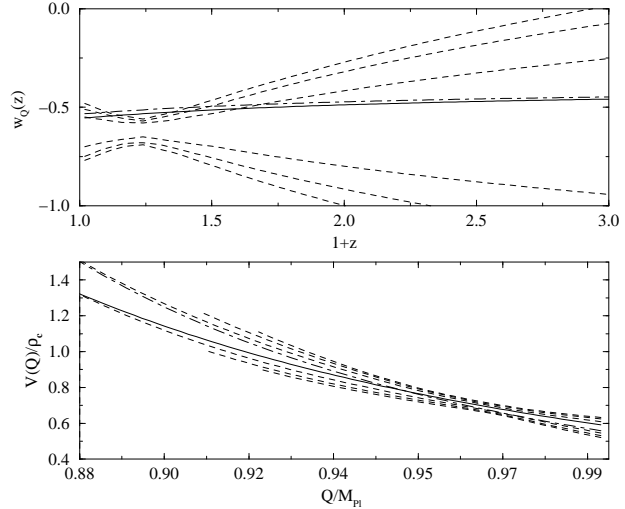


Figure 8. Comparison of models with $V(Q) = M^7/Q^3$ to the confidence contours in Fig. 6. In the lower panel, the dot-dashed line and solid line correspond, respectively, to the minimum and maximum values of M for which the potential falls between the 68% confidence contours. The corresponding lines in the upper panel are $w_Q(z)$ that arise from evolving quintessence in these potentials. Because w_Q decreases monotonically with increasing M for inverse-power-law models, all allowed values of $w_Q(z)$ fall between these two lines. Clearly, models with $V \propto Q^{-3}$ are ruled out by the data.

these could be spurious, the result of unaccounted-for inaccuracies in the fitting function or its derivatives. If we wish to produce useful reconstructions, it will be necessary to use a fitting function similar to equation (13).

Testing individual models as described above could be useful, but because we lack any good theoretical motivation for model-building at present, testing the large numbers of possible models will be very time-consuming. For this reason, it may be more worthwhile to consider more general questions about the dark energy via likelihood analysis in parameter space, rather than to test models individually via reconstruction.

6 PARAMETER ESTIMATION: DETERMINING THE PROPERTIES OF DARK ENERGY

There are two especially important questions we would like to address concerning the properties of the dark energy. First, we would like to know whether the equation of state w_Q differs from -1 —that is, whether the dark energy is the cosmological constant or not—and second, we would like to know whether w_Q varies with redshift. In the previous section, we saw that it is possible to address these questions by performing a likelihood analysis over the parameters $w_Q(0)$, α and Ω_Q . In Fig. 4, we saw that it is possible, for an inverse-power-law quintessence model, to constrain $w_Q(0) \neq -1$ at 95% confidence using SNAP data alone. If we also include prior knowledge of Ω_Q , then it is possible to rule out Λ models at even higher confidence. Even with exact knowledge of Ω_Q , though, it is not possible to rule out $\alpha = 0$ for this

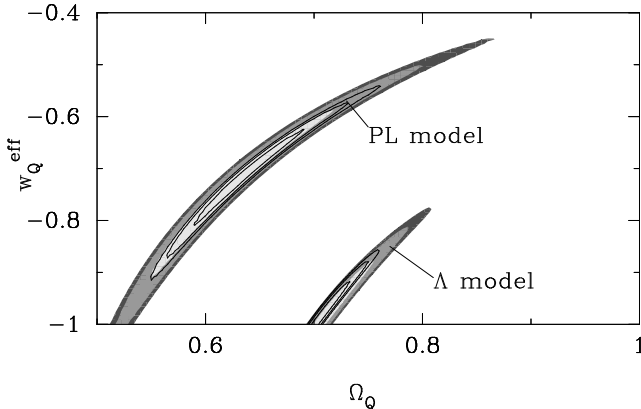


Figure 9. Likelihood contours for Ω_Q and the effective constant equation of state w_Q^{eff} from simulated SNAP data. The contours shown are for an inverse-power-law quintessence model with $V(Q) \propto Q^{-2}$ (“PL model”) and for a cosmological constant model (“ Λ model”). Shaded contours are 68%, 95% and 99% confidence contours for one year of SNAP data (2200 SNe). The line contours define the same confidence regions for three years of data (6600 SNe). Clearly, it is possible to distinguish the quintessence model from a Λ model with high confidence for a full three-year SNAP dataset.

model; it is not possible in this case to say whether w_Q is changing with redshift. This result is in agreement with several previous studies (Astier 2001; Barger & Marfatia 2001; Goliath et al. 2001; Huterer & Turner 2001; Maor et al. 2001; Weller & Albrecht 2001, 2002).

6.1 Two-parameter fits

It is also clear from Fig. 4 that strong degeneracies between α and the other parameters lead to large uncertainties in our parameter estimation. Since we have not been able to say anything particularly useful about α , it might be more useful to leave α out of the analysis entirely for the sake of parameter estimation, focusing our attention on the value of w_Q exclusively. To do this, we derive a fitting function for $\tilde{r}(z)$ based on an effective *constant* equation of state w_Q^{eff} ,

$$\tilde{r}^{\text{fit}}(z) = \int_0^z \frac{dz'}{\left[\Omega_M(1+z')^3 + \Omega_Q(1+z')^{3(1+w_Q^{\text{eff}})} \right]^{1/2}}. \quad (15)$$

Several other authors have considered this parameterization of the coordinate distance, and current supernova observations constrain this parameter to be $w_Q^{\text{eff}} \lesssim -0.4$ (Perlmutter et al. 1999). When these observations are combined with CMB (Efstathiou 1999) or large-scale structure (Perlmutter et al. 1999) data, the constraint becomes $w_Q^{\text{eff}} \lesssim -0.6$. Recently there has been some suggestion that CMB data slightly favors $w_Q^{\text{eff}} > -1$ (Baccigalupi et al. 2002), although this conclusion assumes that some rather poorly constrained parameters are known exactly.

Fig. 9 shows the likelihood contours that are obtained in the parameter space of equation (15) for SNAP-like datasets drawn from a Λ model and a tracker model with potential $V(Q) \propto Q^{-2}$. The figure shows the confidence contours that might be expected for one year and three years of SNAP

data. No priors have been imposed on either of the parameters. In the case of quintessence, with one year of data it is possible to constrain $w_Q^{\text{eff}} \neq -1$ with 68% confidence, and with three years of data it is possible to do so with 99% confidence. Since $w_Q = -1$ for a Λ model, a cosmological constant is ruled out at the same confidence levels. The fact that we can use SNAP to distinguish between a cosmological constant and quintessence is very encouraging. So far, however, we have only shown this for the specific case of an inverse-power-law quintessence model. It is not too surprising that w_Q can be distinguished from -1 in this case, since this model has present-day equation of state $w_Q(0) \approx -0.6$, relatively far from -1 , when $\Omega_Q \approx 0.7$. It will be interesting to see if we can obtain similar results for a broader range of quintessence models—especially those with lower values of w_Q .

To test this, we consider two different tracker potentials. The first is a potential inspired by supergravity (Brax & Martin 1999),

$$V(Q) = \frac{M^{4+P}}{Q^P} \exp \left[\frac{1}{2} \left(\frac{Q}{M_{Pl}} \right)^2 \right]. \quad (16)$$

This potential exhibits tracker behaviour for $P \geq 11$. It also tends to produce lower w_Q than the inverse-power-law potential—for example for $\Omega_Q \approx 0.7$, we have $w_Q(0) \approx -0.8$. We also consider a quintessence model with a potential given by the sum of two power laws,

$$V(Q) = \frac{A}{Q^{P_1}} + \frac{B}{Q^{P_2}} \quad (17)$$

where $P_2 = P_1 \times 10^{-6}$. Because the powers of the two terms differ by six orders of magnitude, this potential tends to produce values for the equation of state that are very close to -1 at the present epoch—when $\Omega_Q \approx 0.7$, we have $w_Q(0) \approx -0.98$. This type of potential was introduced by Steinhardt et al. (1999) to show that a very contrived potential is necessary for a tracker model to produce values of $w_Q(0)$ very close to -1 . We use this potential here to explore the power of SNAP to distinguish quintessence from Λ models in the extreme case when $w_Q(0) \rightarrow -1$. Hereafter, we shall refer to simple inverse-power-law quintessence as a PL model, to the supergravity-inspired quintessence model as a SUGRA model, and to the sum-of-two-power-laws model as a 2PL model.

Fig. 10 shows the likelihood contours that we obtain from SNAP-like datasets drawn from each of these models. In neither case is it possible to constrain $w_Q^{\text{eff}} \neq -1$; hence it is not possible to distinguish either of these models from a cosmological constant using SNAP data alone. (Our results for the Λ , PL, and SUGRA models are in good agreement with the results of Weller & Albrecht (2001, 2002).) Apparently SNAP data, on their own, can only be used to rule out Λ models in cases where w_Q differs significantly from -1 . In section 4, though, we found that applying a prior probability distribution on Ω_Q helped to reduce the errors on all the parameters of our fitting function. Using such prior information might help us to distinguish a larger set of quintessence models from a Λ model. We shall explore this possibility next.

But first we note that there is a discrepancy between our quoted values of Ω_Q and $w_Q(0)$ and the likelihood contours shown in figures 9 and 10. For example, for the

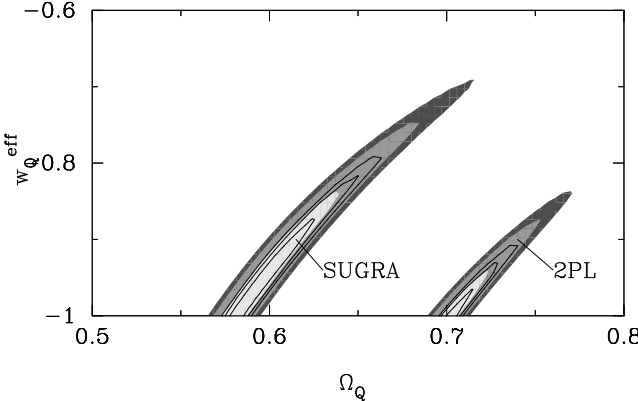


Figure 10. Similar to Fig. 9, except that here the likelihood contours are for data drawn from tracker models arising from the supergravity-inspired potential [“SUGRA”—equation (16)] and the sum of two inverse power laws [“2PL”—equation (17)]. In neither case is it possible, using SNAP data alone, to distinguish the quintessence model in question from a Λ model.

SUGRA model, we get present-day parameters $\Omega_Q \approx 0.7$ and $w_Q(0) \approx 0.8$, but the likelihood analysis gives best-fitting parameters of $\Omega_Q \approx 0.6$ and $w_Q^{eff} \approx -0.95$. Similarly, for the PL model, the actual parameters are $\Omega_Q \approx 0.7$ and $w_Q(0) \approx -0.6$, but the best-fitting parameters are $\Omega_Q \approx 0.6$ and $w_Q^{eff} = -0.7$.

It is important to keep in mind, though, that equation (15) is nothing more than a fitting function to the coordinate distance. In this context, Ω_Q and w_Q^{eff} are merely fitting parameters, and our likelihood analysis simply finds the parameters that produce the best fit to the data. Because our fitting function is only an approximation to $\tilde{r}(z)$, the best-fitting parameters may turn out to be significantly different from the actual physical parameters they represent. (In the present example, the best fit is given by reducing both $w_Q(0)$ and Ω_Q from their actual values.) Nevertheless, these parameters could still be used to rule out a cosmological constant. In the case of a Λ model, the fitting function is an *exact* representation of $\tilde{r}(z)$, so we would expect the best-fit parameters to match the actual parameters. Thus if we rule out $w_Q = -1$, we can say definitively that we are *not* dealing with a Λ model. But it is important to recognize that we can say nothing definitive about the actual values of the parameters, since the best-fit parameters do not necessarily reproduce them.

Now we return to the idea of imposing prior probability distributions on our likelihood analysis. As in section 4, we assume that we have measured $\Omega_M = 1 - \Omega_Q$ with Gaussian error σ_{Ω_M} about its true value. In view of the issues just discussed, it is important to say clearly what we are constraining here. The maximum likelihood parameters in this case are the parameters Ω_Q and w_Q^{eff} that would be most likely to produce the SNAP data if w_Q were constant, given what we already know about Ω_Q . Because we would still expect these most likely parameters to be the correct parameters in the case of a Λ model, ruling out $w_Q^{eff} = -1$ is still tantamount to ruling out the cosmological constant. As shown Figure 11, then, it is possible to rule out a Λ model with 99% confidence for the case of a PL quintessence model, by combining a year of SNAP data and a measurement of

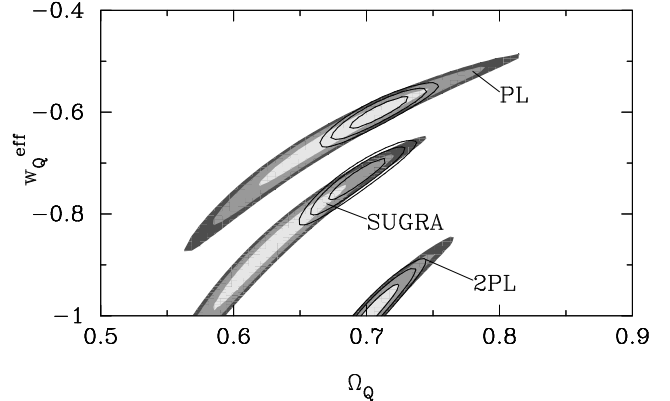


Figure 11. Likelihood contours in Ω_Q - w_Q^{eff} space for various quintessence models, assuming Gaussian prior probability distributions on $\Omega_M = 1 - \Omega_Q$. The shaded contours indicate 68%, 95% and 99% confidence levels assuming a prior with standard deviation $\sigma_{\Omega_M} = 0.05$, and the line contours define the same confidence regions for $\sigma_{\Omega_M} = 0.015$. All contours use a one-year SNAP dataset. Including such priors in our analysis allows us to distinguish the PL and SUGRA models from a cosmological constant, but they provide no discriminatory power in the case of the 2PL model.

Ω_M with $\sigma_{\Omega_M} = 0.05$. In the case of the SUGRA model, we can rule out the cosmological constant at 99% confidence if we have $\sigma_{\Omega_M} = 0.015$. This is encouraging: it appears that using SNAP in concert with other cosmological observations will provide a strong test of the basic properties of dark energy.

It is important to note, however, that the data cannot distinguish the 2PL quintessence model from a cosmological constant model, even with a very good measurement of Ω_M . Although this model is highly contrived, it is clear that SNAP will not be able to distinguish any arbitrary quintessence model from a Λ model using equation (15) as a fitting function. As w_Q approaches -1 , quintessence becomes increasingly difficult to distinguish from a cosmological constant model, and our only hope for distinguishing quintessence from Λ is to probe the evolution of w_Q with redshift.

6.2 Three-parameter fits

To probe the evolution of w_Q with redshift, we return to the three-parameter fitting function that we used previously for reconstruction, equation (13), which was based on the approximate equation of state $w_Q^{app}(z) = w_Q(0) - \alpha \ln(1 + z)$. As we saw in Fig. 4, to get a tight constraint on α it was necessary to impose a Gaussian prior on Ω_M with an optimistic value for σ_{Ω_M} of something like 0.015. Fig. 12 shows the likelihood contours that would be expected for one and three years of SNAP data combined with such a prior. We consider the same three quintessence models as before. Only in the case of the SUGRA model is it possible to constrain α to be nonzero—and here only at 68% confidence, and only for a full, three-year dataset.

It is hardly surprising that $\alpha \neq 0$ is more readily shown for the SUGRA model. In this model, w_Q is evolving relatively rapidly at late times, with $\alpha = -0.43$, as opposed

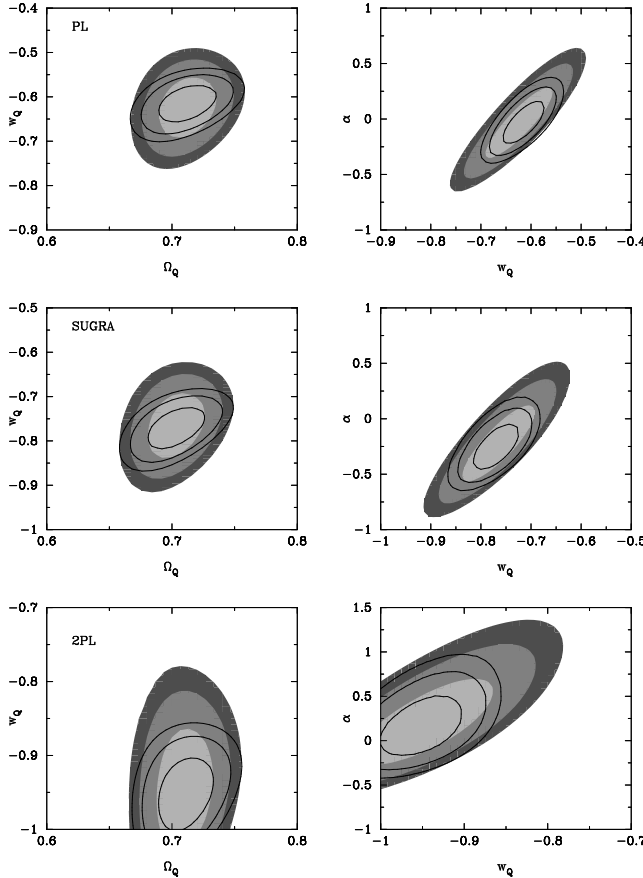


Figure 12. Likelihood contours for the parameters Ω_Q , w_Q and α , as defined in equation (13). The contours shown are for, from top to bottom, the PL, SUGRA and 2PL models. The shaded contours are for one year of SNAP data and the line contours are for three years of data, where in each case a Gaussian prior with $\sigma_{\Omega_M} = 0.015$ has been imposed on $\Omega_M = 1 - \Omega_Q$. Only in the case of the SUGRA model is it possible to constrain α to be nonzero at any significant confidence level, and then only for a full, three-year dataset.

to -0.11 for the PL model and -0.01 for the 2PL model. Clearly, SNAP will be much less powerful for distinguishing evolving from non-evolving dark energy models than it is for distinguishing quintessence from Λ models. In most cases, then, it appears that two-parameter fitting functions will be more useful than three-parameter fitting functions for constraining cosmology with supernova data.

7 LONG-TERM PROSPECTS FOR PROBING QUINTESSENCE

So far we have seen that SNAP will be a powerful tool for determining properties of the dark energy. But even with very good prior information, it may not be possible to distinguish between two very similar-looking models, such as a 2PL model and a Λ model. It has been shown that supernova data do a better job of constraining some cosmological parameters when the survey is extended to higher redshifts, $z > 2$ (Efstathiou 1999). Although SNAP will only track supernovae out to redshifts of $z = 1.7$, it could be possible in

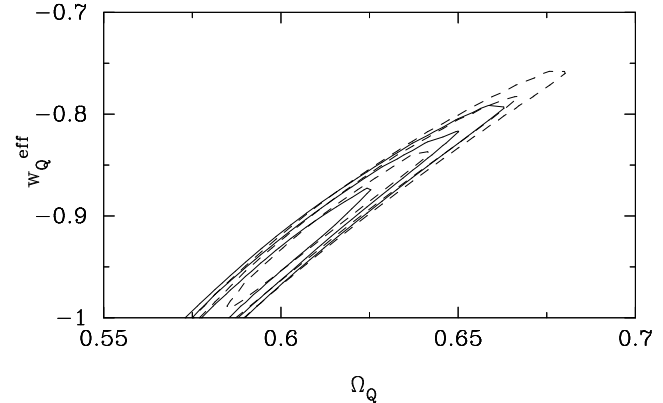


Figure 13. Likelihood contours in Ω_Q - w_Q^{eff} space for the SUGRA quintessence model. Solid contours define 68%, 95% and 99% confidence levels for three years of SNAP data, and dashed lines define the same regions when that data is supplemented by a sample of 30 supernovae at redshift $z = 3$. When the high-redshift sample is included, it is possible to rule out a Λ model ($w_Q^{eff} = -1$) with 68% confidence. No prior knowledge of the parameters is assumed in either case.

the long term to supplement SNAP data with higher-redshift data from powerful new telescopes like the Next Generation Space Telescope (NGST). To get some rough idea of the usefulness of such observations, we simulate them by adding a sample of 30 supernovae at redshift $z = 3$ to our SNAP-like datasets.

Fig. 13 shows the improvement that can be made on a two-parameter likelihood analysis for the SUGRA model, when we supplement SNAP data with high-redshift observations. Whereas previously it was impossible to rule out a Λ model using SNAP data alone, as shown in Fig. 13, when we supplement a three-year SNAP dataset with high-redshift supernovae, we can rule out a Λ model with 68% confidence, with no prior knowledge of the parameters. We see a similar shift in the confidence regions for the PL and 2PL models, although the 2PL model still cannot be distinguished from a Λ model.

In the case of a three-parameter fit, the effect of adding a high-redshift sample is smaller, but it can still be important in some cases. Fig. 14 shows the likelihood contours that would be expected in the case of the 2PL quintessence model, for a three-parameter fit to a three-year dataset, imposing a Gaussian prior on Ω_M with $\sigma_{\Omega_M} = 0.015$. The high-redshift observations do not affect the confidence contours strongly enough to indicate a nonzero α , but they do constrain $w_Q(0) \neq -1$ at 68% confidence, ruling out a Λ model at that confidence level. Obtaining this result is somewhat surprising, since it was not possible to do so with a two-parameter fit. The reason it is possible here is that, since our three-parameter fitting function allows w_Q to vary with z , the parameters $w_Q(0)$ and Ω_Q are likely to be more accurately constrained, whereas the two-parameter fit required an offset in the best-fit parameters to make up for the z -dependence of w_Q . Three-parameter fitting functions, then, may be more useful than two-parameter fitting functions in some cases, even when they cannot be used to discern the evolution of w_Q .

Finally, we note that Fig. 14 assumes a very optimistic

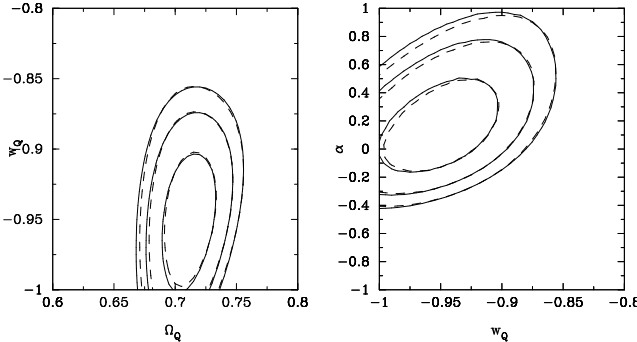


Figure 14. Likelihood contours for a three-parameter fit to SNAP-like data drawn from a 2PL quintessence model. Solid contours are for three years of SNAP data; dashed contours are for a three-year dataset supplemented with 30 supernovae at $z = 3$. With the high-redshift sample, it is possible to distinguish the 2PL model from a Λ model.

observational scenario. To distinguish the 2PL model from a Λ model, we must have three years of SNAP data with negligible systematic errors, plus thirty high-redshift supernovae from NGST, an independent measurement of Ω_M with $\sim 5\%$ errors, and extremely good evidence that the universe is flat. But although an observational programme that would lead to constraints like those in Fig. 14 is ambitious, it is certainly not impossible. The simulated SNAP dataset we used in this analysis has realistic statistical errors, and systematics are expected to be negligible in comparison (Levi et al. 2000). NGST, when launched, will almost certainly see at least some additional high-redshift supernovae. Also, as we have noted, our assumed prior constraints on Ω_M are realistic. Furthermore, the MAP and Planck satellites should provide very precise measurements of the curvature of the universe [to within a percent or so for Planck (Tauber et al. 2000)]. The first steps have been taken toward observations that could lead to a measurement like Fig. 14. Although this figure represents a best-case scenario, it also represents an achievable long-term goal.

8 CONCLUSION

In this study we have investigated the prospects for probing the dark energy, particularly quintessence, with observations of type Ia supernovae. We have examined tests for individual quintessence models (reconstruction) as well as tests that address more general questions about the dark energy (parameter estimation by likelihood analysis). In both cases, we find that data from the proposed SNAP satellite will provide important information about dark energy, either alone or when combined with other cosmological observations.

In the case of reconstruction it will be important to take extreme care in choosing a function to fit SNAP's measurement of the distance-redshift relation $r(z)$. By using a fitting function based on a physical approximation to the coordinate distance, it is possible to produce accurate and reliable reconstructions from SNAP data combined with independent cosmological observations. Such reconstructions might provide useful observational constraints as we construct models for the dark energy.

To answer our basic questions about the nature of the dark energy, however, cosmological parameter estimation may be more useful. If the dark energy equation of state is significantly different from -1 , the SNAP data alone will be able to rule out the cosmological constant. Moreover, combining the SNAP constraints with independent measurements of Ω_M will allow us to rule out Λ models for all but the most extreme cases of quintessence, when w_Q is very close to -1 . SNIa are less likely to provide evidence that w_Q is evolving. Even combining SNAP data with very precise measurements of Ω_M will only provide evidence of an evolving w_Q in cases of extremely strong evolution. Three-parameter fits may still be useful, however: because they allow a more accurate determination of $w_Q(0)$ than two-parameter fits, they may be able to rule out a cosmological constant in cases where a two-parameter fit cannot do so.

The prospects are good for probing dark energy with SNIa data. SNAP, by itself, may be able to constrain cosmological parameters with enough precision to rule out the cosmological constant as a dark energy candidate. However, it is when SNIa data are combined with other observations that their true value becomes apparent. When combined with expected future measurements of Ω_M , for example, SNAP data provide much stronger constraints on the quintessence equation of state and may be able to produce useful reconstructions of the equation of state and quintessence potential. In each of these cases, the combination of several observations tells us much more than any of the observations by itself, and in each case, the SNIa observations are an essential component. The measurements that may answer our questions about dark energy over the next decade or two constitute a difficult and impressive observational programme. Improved supernova observations are crucial to its success.

ACKNOWLEDGMENTS

BFG acknowledges the generous support of the Herchel Smith fellowship from Williams College, USA.

REFERENCES

- Armendariz C., Mukhanov V., Steinhardt P., 2000, PRL, 85, 4438
- Armendariz C., Mukhanov V., Steinhardt P., 2001, PRD, 63, 103510
- Astier P., 2001, Phys. Lett. B, 500, 8
- Baccigalupi et al., 2002, PRD, 65, 063520
- Barger V., Marfatia D., 2001, Phys. Lett. B, 498, 67
- Bean R., 2001, PRD, 64, 123516
- Bean R., Melchiorri A., 2002, PRD, 65, 041302
- Brax P., Martin J., 1999, Phys. Lett. B, 468, 40
- Caldwell R., Dave R., Steinhardt P. J., 1998, PRL, 80, 1582
- Chiba T., Nakamura T., 2000, PRD, 62, 121301
- Corasaniti P., Copeland E., 2002, PRD, 65, 043004
- de Bernardis P., et al., 2002, ApJ, 564, 559
- Efstathiou G., 1999, MNRAS, 310, 842
- Efstathiou G., et al., 1999, MNRAS, 303, L47
- Efstathiou G., et al., 2002, MNRAS, 330, L29
- Eisenstein D., Hu W., Tegmark M., 1998, ApJ, 504, L57
- Goliath M., et al., 2001, A&A, 380, 6

- Haiman Z., Mohr J., Holder G., 2001, ApJ, 553, 545
Hu W., et al., 1998, PRD, 59, 023512
Huterer D., Turner M., 1999, PRD, 60, 081301
Huterer D., Turner M., 2001, PRD, 64, 123527
Levi M., et al., 2000, <http://snap.lbl.gov>
Maor I., Brustein R., Steinhardt P., 2001, PRL, 86, 6
Nakamura T., Chiba T., 1999, MNRAS, 306, 696
Netterfield C., et al., 2002, ApJ
Peebles P. J. E., Ratra B., 1988, ApJ, 325, L17
Perlmutter S., et al., 1999, ApJ, 517, 565
Perlmutter S., Turner M., White M., 1999, PRL, 83, 670
Pryke C., et al., 2002, astro-ph/0104490
Riess A., et al., 1998, AJ, 116, 1009
Saini T., et al., 2000, PRL, 85, 1162
Starobinsky A., 1998, JETP Lett., 68, 757
Steinhardt P., Wang L., Zlatev I., 1999, PRD, 59, 123504
Tauber J., et al., 2000, <http://astro.estec.esa.nl/SA-general/Projects/Planck>
van Waerbecke L., Bernardeau F., Mellier Y., 1999, A&A, 342, 15
Vilenkin A., 2001, hep-th/0106083
Wang X., Tegmark M., Zaldarriaga M., 2002, PRD
Wang Y., Garnavich P. M., 2001, ApJ, 552, 445
Wang Y., Lovelace G., 2001, ApJ, 562, L115
Weller J., Albrecht A., 2001, PRD, 86, 1939
Weller J., Albrecht A., 2002, PRD
Weller J., Battye R., Kneissl R., 2001, astro-ph/0110353
Zlatev I., Wang L., Steinhardt P., 1999, PRL, 82, 896